STEVEN C. WILHELMS

Environmental & Water Quality Operational Studies

TECHNICAL REPORT E-81-10

GAS TRANSFER IN HYDRAULIC JUMPS

By Steven C. Wilhelms, Lancelot Clark,
James R. Wallace

School of Civil Engineering
Georgia Institute of Technology
Atlanta, Ga. 30332

and Dennis R. Smith

Hydraulics Laboratory
U. S. Army Engineer Waterways Experiment Station
P. O. Box 631, Vicksburg, Miss. 39180

July 1981

Final Report

Approved for Public Release; Distribution Unlimited

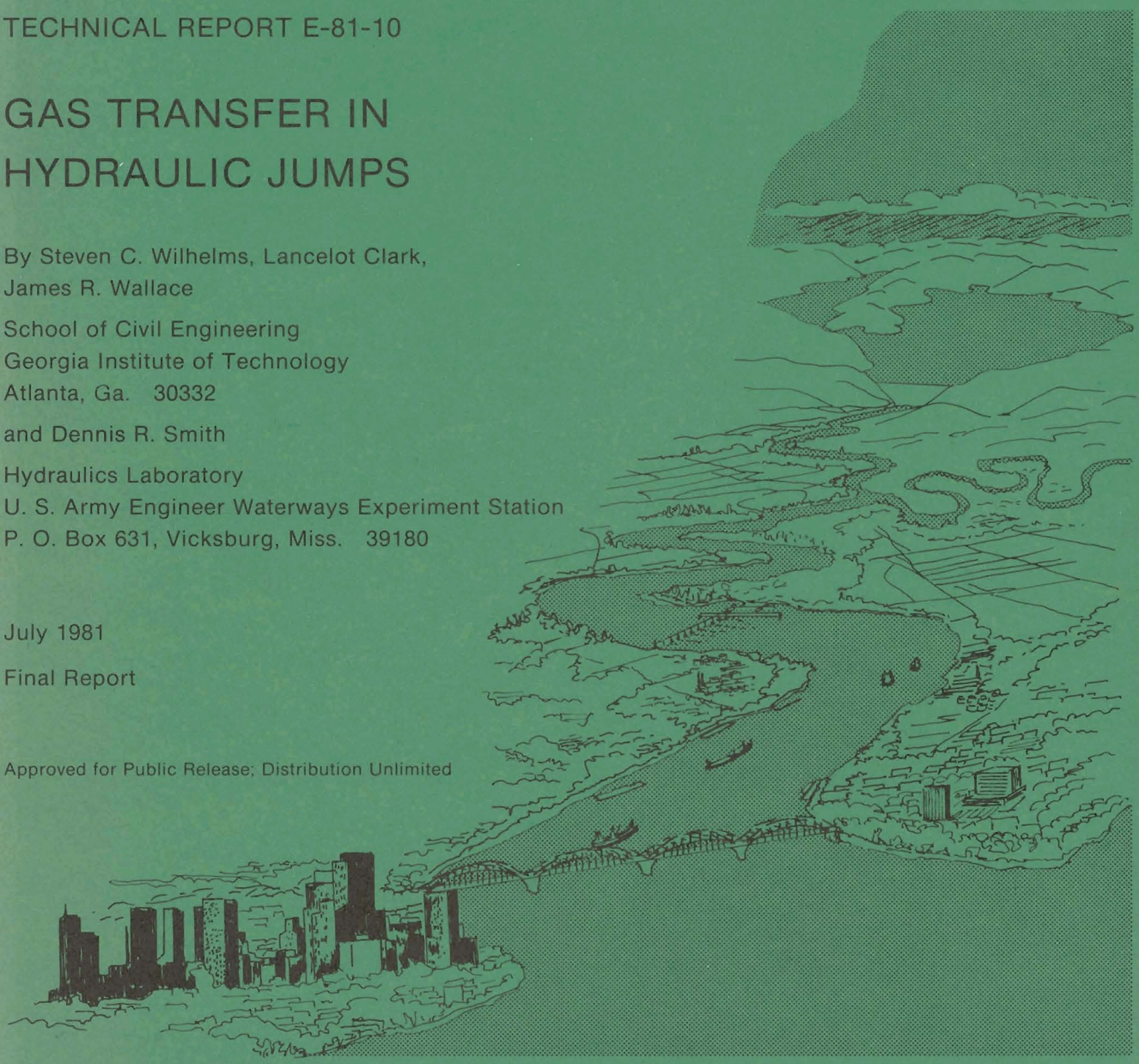

Prepared for Office, Chief of Engineers, U. S. Army
Washington, D. C. 20314

Under Contract No. DACW39-77-C-0079
(EWQOS Work Unit III A.2)

Monitored by Hydraulics Laboratory
U. S. Army Engineer Waterways Experiment Station
P. O. Box 631, Vicksburg, Miss. 39180

Unclassified

SECURITY CLASSIFICATION OF THIS PAGE (When Data Entered)

REPORT DOCUMENTATION PAGE

READ INSTRUCTIONS BEFORE COMPLETING FORM

1. REPORT NUMBER
Technical Report E-81-10

2. GOVT ACCESSION NO.

3. RECIPIENT'S CATALOG NUMBER

4. TITLE (and Subtitle)
GAS TRANSFER IN HYDRAULIC JUMPS

5. TYPE OF REPORT & PERIOD COVERED
Final report

6. PERFORMING ORG. REPORT NUMBER

7. AUTHOR(s)
Steven C. Wilhelms, Lancelot Clark, James R. Wallace, and Dennis R. Smith

8. CONTRACT OR GRANT NUMBER(s)
Contract No. DACW-39-77-C-0079

9. PERFORMING ORGANIZATION NAME AND ADDRESS
School of Civil Engineering, Georgia Institute of Technology, Atlanta, Ga. 30332 and
U. S. Army Engineer Waterways Experiment Station Hydraulics Laboratory, P. O. Box 631, Vicksburg, Miss. 39180

10. PROGRAM ELEMENT, PROJECT, TASK AREA & WORK UNIT NUMBERS
EWQOS Work Unit III A.2

12. REPORT DATE
July 1981

13. NUMBER OF PAGES
50

11. CONTROLLING OFFICE NAME AND ADDRESS
Office, Chief of Engineers, U. S. Army
Washington, D. C. 20314

14. MONITORING AGENCY NAME & ADDRESS(if different from Controlling Office)
U. S. Army Engineer Waterways Experiment Station
Hydraulics Laboratory
P. O. Box 631, Vicksburg, Miss. 39180

15. SECURITY CLASS. (of this report)
Unclassified

15a. DECLASSIFICATION/DOWNGRADING SCHEDULE

16. DISTRIBUTION STATEMENT (of this Report)

Approved for public release; distribution unlimited.

17. DISTRIBUTION STATEMENT (of the abstract entered in Block 20, if different from Report)

18. SUPPLEMENTARY NOTES
Available from National Technical Information Service, 5285 Port Royal Road, Springfield, Va. 22151.

19. KEY WORDS (Continue on reverse side if necessary and identify by block number)
Gases
Hydraulic jump
Radioactive tracers

20. ABSTRACT (Continue on reverse side if necessary and identify by block number)

A radioactive tracer technique was employed to evaluate the gas transfer occurring in hydraulic jumps characterized by a range of Froude numbers. Various relationships of gas transfer to Froude number, unit discharge, and Reynolds number are formulated and presented. These relationships are compared with other experimenter's work in the same area. Conclusions are drawn regarding applicability to prototype predictions or evaluations of gas transfer.

DD FORM 1 JAN 73 1473 EDITION OF 1 NOV 65 IS OBSOLETE

Unclassified

SECURITY CLASSIFICATION OF THIS PAGE (When Data Entered)

PREFACE

This investigation was conducted as part of the Environmental and Water Quality Operational Studies (EWQOS) Program sponsored by the Office, Chief of Engineers, U. S. Army. The EWQOS Program is being administered by the Environmental Laboratory (EL) of the U. S. Army Engineer Waterways Experiment Station (WES), Vicksburg, Miss. This contract was monitored by the Hydraulic Structures Division (HS), Hydraulics Laboratory (HL), under the direction of Messrs. H. B. Simmons, Chief of HL and J. L. Grace, Jr., Chief of HS.

The investigation was conducted at the Georgia Institute of Technology, School of Civil Engineering, during the period October 1977 to September 1978 under Contract No. DACW-39-77-C-0079 in EWQOS Work Unit III A.2. The investigation was under the supervision of Dr. James R. Wallace, Associate Professor of Civil Engineering. In partial fulfillment of the requirements for Masters of Science degrees in Civil Engineering, Messrs. Steven C. Wilhelms and Lancelot Clark conducted the experiments. Also assisting in the testing and analysis were Messrs. G. P. Utterbeck, L. M. Rennell, P. J. Mitchell, A. C. Waite, R. Starr, J. Ramos, S. Kwabbi, M. Holmes, and Mrs. S. M. Wilhelms. The report was prepared by Messrs. Wilhelms and Clark and was reviewed by Dr. Wallace and Dr. Dennis R. Smith, Chief of the Reservoir Water Quality Branch, HL, WES.

During the investigation, Dr. Jerome L. Mahloch was Program Manager of the EWQOS Program, Dr. John Harrison was Chief of EL, and Mr. H. B. Simmons was Chief of HL.

COL John L. Cannon, CE, and COL Nelson P. Conover, CE, were Commanders and Directors of WES during the investigation. Mr. Fred R. Brown was Technical Director.

This report should be cited as follows:

> Wilhelms, S. C., Clark, L., Wallace, J. R., and Smith, D. R. 1981. "Gas Transfer in Hydraulic Jumps," Technical Report E-81-10, U. S. Army Engineer Waterways Experiment Station, CE, Vicksburg, Miss.

CONTENTS

	Page
PREFACE	1
CONVERSION FACTORS, U. S. CUSTOMARY TO METRIC (SI) UNITS OF MEASUREMENT	3
PART I: INTRODUCTION	4
Background	4
Objective	5
Scope	5
PART II: METHODOLOGY	7
Tracer Technique	7
Testing Facilities	11
PART III: TESTING	15
Hydraulic Conditions	15
Procedure	18
Analysis	23
PART IV: RESULTS	24
PART V: DISCUSSION	28
PART VI: CONCLUSIONS AND RECOMMENDATIONS	33
REFERENCES	39
APPENDIX A: KRYPTON-TO-DYE RATIOS AND PERTINENT DATA FOR HYDRAULIC JUMPS	A1

CONVERSION FACTORS, U. S. CUSTOMARY TO METRIC (SI) UNITS OF MEASUREMENT

U. S. customary units of measurement used in this report can be converted to metric (SI) units as follows:

Multiply	By	To Obtain
cubic feet per second	0.0283168	cubic metres per second
feet	0.3048	metres
feet per second	0.3048	metres per second
feet per second per second	0.3048	metres per second per second
inches	2.54	centimetres

GAS TRANSFER IN HYDRAULIC JUMPS

PART I: INTRODUCTION

Background

1. During thermal stratification of lakes, oxygen stratification may also occur. Typically, the dissolved oxygen (DO) is high in the upper regions near the surface of the lake (epilimnion), decreases in the thermocline region (where temperature gradient is largest, metalimnion), and is low or zero in the lower region of the lake (hypolimnion). Depending upon the depth of withdrawal, releases from the lake may have low or zero DO. Because many kinds of aquatic life cannot survive in a low DO environment, it is necessary to evaluate and describe the various reoxygenation processes so that release structures may be designed to enhance release DO.

2. One reoxygenation process is reaeration. It is the direct absorption of oxygen from the atmosphere and can be considered as two physical processes working together: molecular diffusion from the atmosphere across the air/water interface and subsequent dispersion throughout the water due to turbulence and molecular diffusion. In most hydraulic systems, including hydraulic structures, turbulent dispersion is the dominant process determining the rate of reaeration.

3. Turbulence is an extremely complex process and is influenced by the physical properties of the fluid, the geometry of the system, and the characteristics of flow. The complex combination of these factors essentially precludes accurate measurement and mapping of turbulence in the flow fields typically encountered in hydraulic structures. As a result it has not been possible to directly relate reaeration to turbulence. The Federal Water Pollution Control Administration developed a procedure for directly and accurately measuring the gas transfer capacity of flowing water (Tsivoglou et al. 1965). The technique, which employs a gaseous tracer, has been successfully applied to numerous streams (Tsivoglou et al. 1968; Tsivoglou 1967; Tsivoglou and

Wallace 1972) and is becoming accepted as one of the most accurate methods (Rathbun 1977) available for determining reaeration rates. However, the technique has been applied mostly to streams flowing in natural channels, leaving essentially untouched the subject of reaeration in man-made structures such as stilling basins below dams or other reservoir outlet structures.

4. To develop generalized predictive techniques for reaeration, it will be necessary to identify and analyze the reaeration occurring in the various flow regimes encountered in a hydraulic structure. If the gas transfer occurring in each flow regime can be related to hydraulic, geometric, and/or kinematic features, it may be possible to physically or mathematically model the total gas transfer occurring in the structure by simple superposition. The tracer technique provides the means for accurately measuring the reaeration which occurs in the various reaches and flow regimes of a hydraulic structure. By making these measurements in structure prototypes and models, the relationships mentioned may be developed. Once these relationships are known, it may be possible to develop techniques that would permit prediction of prototype gas transfer based on measurements made in a hydraulic model.

5. Hydraulic jumps are flow phenomena that are part of the energy dissipation design at many hydraulic structures. Because of this prevalence, the gas transfer in hydraulic jumps was evaluated using the radioactive tracer technique. The results of the study are reported herein.

Objective

6. The objective of this study was to investigate the gas transfer characteristics of hydraulic jumps and examine relationships which might provide a basis for quantifying the reaeration rates or gas losses.

Scope

7. The gas transfer occurring in several hydraulic jumps with

Froude numbers ranging from 1.5 to 9.5 was measured with a gaseous tracer technique. Unit discharges of 0.261, 0.330, and 0.462 cfs* per foot were tested for the stated Froude number range. The relationships of gas transfer, Froude number, unit discharge, and Reynolds number were examined.

---

* A table of factors for converting U.S. customary units of measurement to metric (SI) units is presented on page 3.

PART II: METHODOLOGY

Tracer Technique

8. The gaseous tracer method utilized in this study involves two tracers simultaneously and continuously injected into the flow at a steady rate. Krypton-85 (kr-85), as a dissolved gas, was the tracer for dissolved oxygen. Rhodamine-WT fluorescent dye was the tracer for dispersion.

9. At equilibrium, gas concentration in water is linearly dependent upon the partial pressure of the gas in the overlying atmosphere. Henry's Law states

$$C_s = Kp$$

where

C_s = saturation concentration
p = partial pressure of the gas in the atmosphere
K = proportionality constant

In the saturated condition, there is no net gas transfer across the air/water interface since the partial pressure of the gas in the water is in equilibrium with the partial pressure of the gas in the atmosphere. If the gas concentration in the water is different from the saturation concentration, the partial pressure of the gas in the water and atmosphere is unequal. This results in a force causing the absorption or desorption of the gas until equilibrium is established. For oxygen, if the actual concentration is less than saturation, the "saturation deficit" is defined by

$$D = \left| C_s - C \right|_{ox} \tag{1}$$

where

D = saturation deficit
C = concentration in the water

10. As long as the concentration of oxygen in the water is less than the saturation concentration, there will be a net movement of

oxygen from the atmosphere to the water. The rate of change of the saturation deficit at any time is proportional to the deficit at that time, or, the greater the deficit, the greater the rate of oxygen transfer. This process can be represented by

$$\frac{dD}{dt} = -K_{ox}D \tag{2}$$

where

t = time

K_{ox} = a proportionality constant referred to as the "reaeration rate coefficient"

11. If there were no sources or sinks or factors other than reaeration affecting the oxygen concentration, integrating Equation 2 would provide a means for determining the proportionality constant, K_{ox}, through the relationship

$$D = D_o \exp(-K_{ox}t) \tag{3}$$

where

D_o = saturation deficit at some initial time, $(t = 0)$

D = saturation deficit at some later time t

There are many chemical and biological processes which can affect DO in natural systems; therefore, to measure the reaeration coefficient it is necessary to use an inert gas as the tracer so that no gas is lost through such processes. The radioactive tracer technique meets this requirement.

12. The concentration of krypton-85 tracer gas in the water is analogous to the saturation deficit,

$$C = \left| C_s - C \right|_{kr}$$

C_s for krypton-85 is zero since the partial pressure of krypton-85 in the atmosphere is essentially zero (Henry's Law). There will be a

continuous loss of the gas to the atmosphere until equilibrium is achieved and the krypton-85 concentration is reduced to zero. Thus the gas loss process for krypton-85 is mathematically described by

$$C = C_o \exp(-K_{kr} t) \tag{4}$$

where

C_o = concentration of kr-85 at some initial time, $(t = 0)$
C = concentration of kr-85 remaining in the water at some later time, t

which is identical in form to Equation 3, the description of the oxygen transfer process. Since krypton gas is inert, it is not subject to the chemical and biological processes which affect oxygen. This makes it possible to compute, through Equation 4, a gas exchange coefficient for krypton, K_{kr}, which reflects gas transfer independent of chemical or biological effects.

13. It has been shown that the ratio of exchange coefficients for these two gases is equal to a constant (Tsivoglou and Wallace 1972)

$$\frac{K_{kr}}{K_{ox}} = 0.83 \pm 0.04 \tag{5}$$

where

K_{kr} = exchange coefficient for krypton
K_{ox} = exchange coefficient for oxygen

This relationship is not significantly affected by temperature (within the range of interest), degree of turbulent mixing, or the direction of gas transfer. This makes possible the calculation of K_{kr} from Equation 4 and subsequent determination of K_{ox} with Equation 5.

14. Consider two points A and B which lie on a natural system such as a stream or channel. Let A be the upstream point and let a quantity of dissolved krypton gas be introduced upstream of A. If the tracer gas were introduced uniformly across the cross-sectional flow area and there were no vertical or horizontal velocity gradients in the

flow causing dispersion, and if there were no tributaries to cause dilution, then the exchange coefficient of krypton-85, K_{kr}, between points A and B could be calculated from Equation 4 in the form

$$\frac{C_B}{C_A} = \exp(-K_{kr}t) \tag{6}$$

where

C_A, C_B = krypton gas concentration at stations A and B
t = time-of-travel from A to B

15. Since dilution and dispersion are present, they must be considered. A correction which accounts for dispersion and dilution may be applied to Equation 6 by using flourescent dye concentrations. The fluorescent dye, in solution in the tracer mixture, is released simultaneously with the krypton gas. Since the tracers are injected simultaneously, the krypton-85 undergoes the same dispersion and dilution as the dye. Using the observed dye concentrations and krypton-85 concentrations, the krypton exchange coefficient, K_{kr}, can be calculated by

$$\frac{\left(\frac{C_{kr}}{C_D}\right)_B}{\left(\frac{C_{kr}}{C_D}\right)_A} = \exp\,(-K_{kr}t) \tag{7}$$

where

$\left(\frac{C_{kr}}{C_D}\right)_A$, $\left(\frac{C_{kr}}{C_D}\right)_B$ = ratios of krypton concentration to dye concentration at points A and B
t = time of flow from A to B

With flow conditions such as those in these tests, the amount of dye which might be adsorbed on the flume or otherwise lost was assumed to be insignificant.

16. In the present study the two tracers are mixed together and injected simultaneously. Samples taken from the flow at stations A and B are analyzed in a liquid scintillation counter for krypton-85 content

and in a fluorometer for dye content. The travel time is obtained from brine (conductivity) tests described in paragraph 24. The observed data thus permit the calculation of the krypton exchange coefficient, K_{kr}, and subsequent determination of K_{ox} for the reach AB.

Testing Facilities

Description

17. The flume used in this study was glass-walled and 1.25 ft wide with a maximum flow of 0.6 cfs (Figure 1). A vertical sluice gate was used to control the depth of water in the headbay, thus controlling the velocity of the flow upstream of the hydraulic jump. A tailgate varied the tailwater depth creating the necessary sequent depth which caused a hydraulic jump to occur in the flume. The flow in the flume was determined with a calibrated elbow meter and manometer.

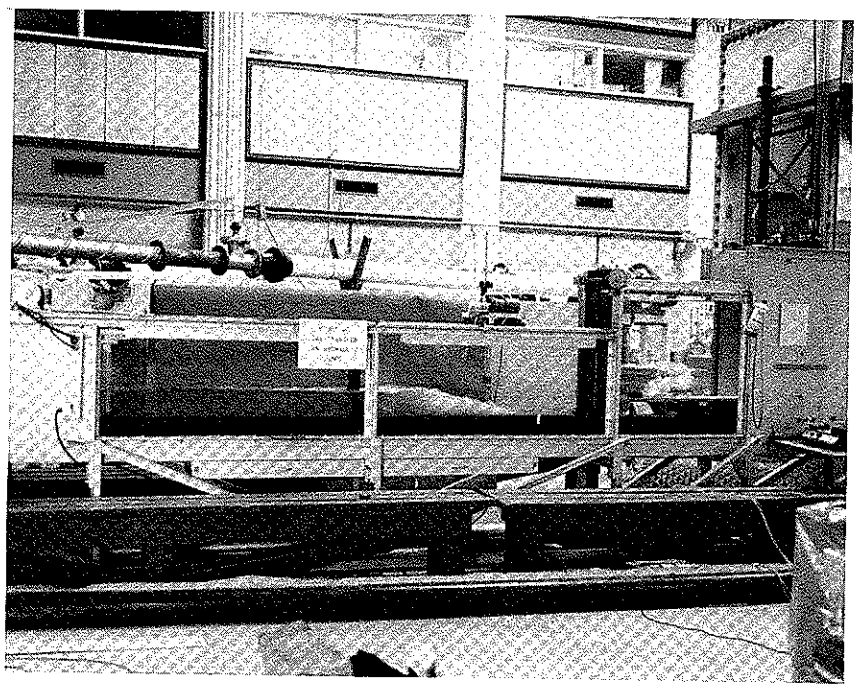

Figure 1. Testing facilities

Procedure

18. Water samples were collected at two depths using two Masterflex tubing pumps. Both pumps were driven by the same motor to assure

that their pumping rates were identical. The sample intakes were 1/4 in. stainless steel tubes connected to tygon tubing leading to pumps (Figure 2). Care was exercised to obtain identical lengths of tubing in the sampling system to assure simultaneous sampling.

19. The radioactive dose (krypton-85 and dye) was injected continuously into the headbay with a precision syringe pump (Figure 3).

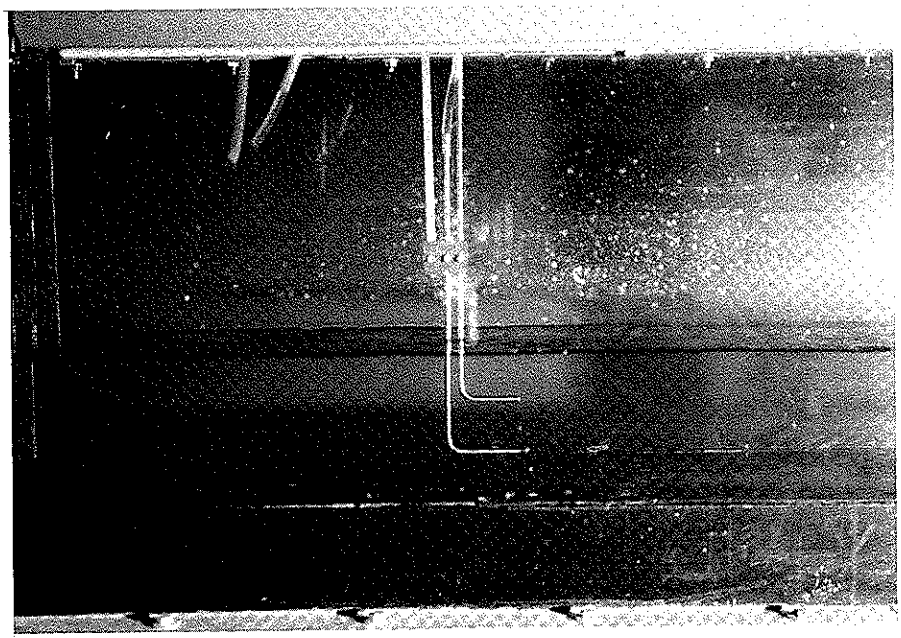

Figure 2. Sampler intakes

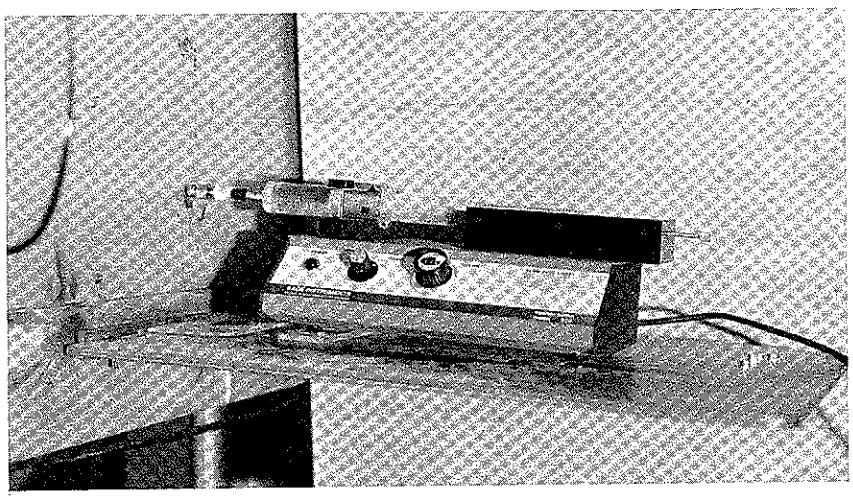

Figure 3. Precision syringe pump

The injection location was just upstream of a Venturi section placed in the headbay (Figure 4). A 1/8-inch-diameter stainless steel tube with three small holes (0.0156-inch-diameter) was used as a manifold to distribute the dose across the width of flow. The dosed water then flowed through a confined section to the sluice gate. This prevented gas loss upstream of the sluice gate.

20. The entire flume was covered with a blower placed at the downstream end of the flume which allowed the air space above the flowing water to be exhausted to the atmosphere outside the lab. This prevented any buildup of radioactive gas in the laboratory.

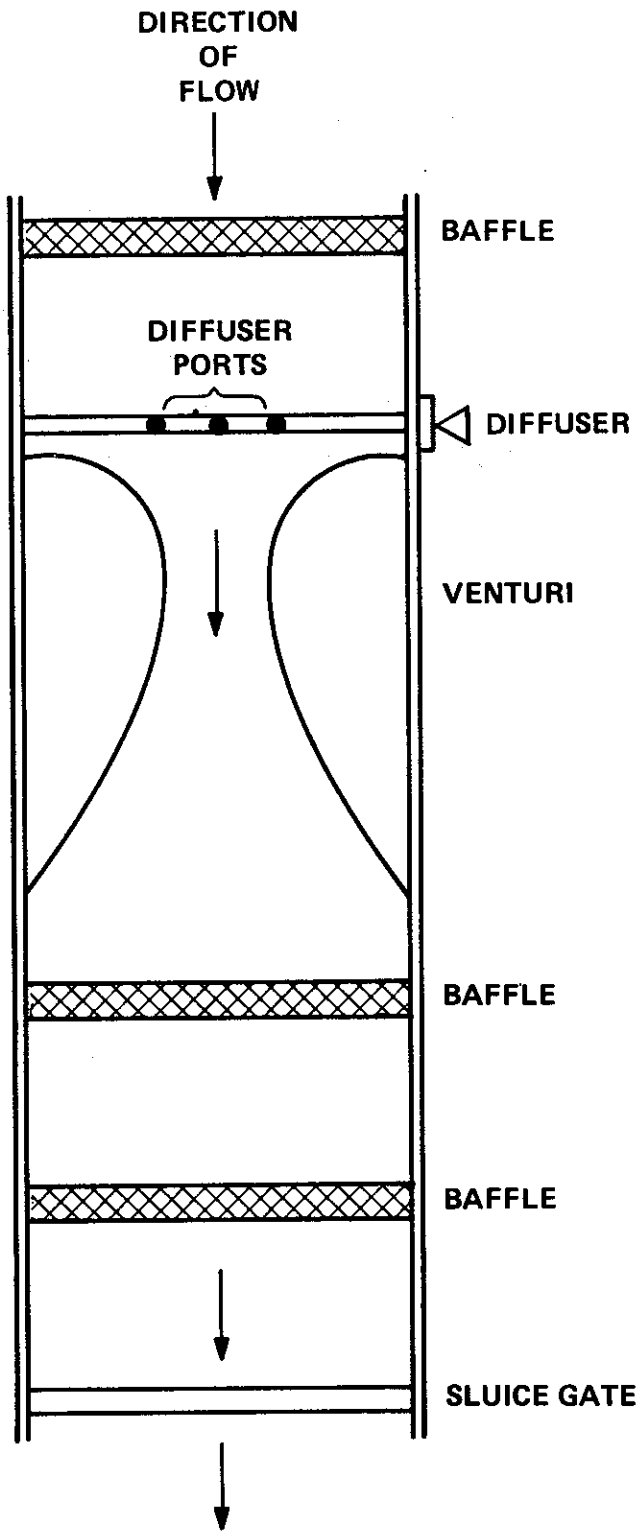

Figure 4. Venturi and diffuser upstream of sluice gate

PART III: TESTING

Hydraulic Conditions

21. The hydraulic jumps tested encompassed four ranges of Froude numbers and were classified (Chow 1959) in the following manner:

Froude Number	Jump Classification
1.0 to 1.7	Undulating
1.7 to 2.5	Weak
2.5 to 4.5	Oscillating
4.5 to 9.0	Steady

Hydraulic jumps with flow characteristics of each class were studied. Figure 5 shows a hydraulic jump with a Froude number, F = 9.3. Figures 6, 7, 8, and 9 show jumps with Froude numbers of 5.9, 3.3, 2.4, and 1.8, respectively. These figures illustrate the different jumps tested

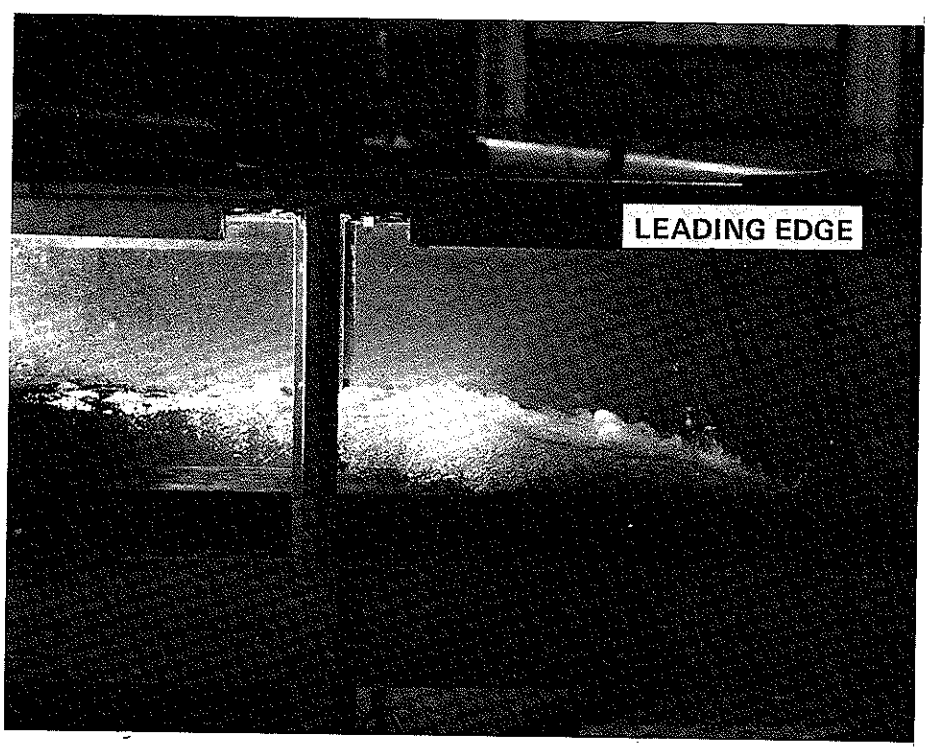

Figure 5. Hydraulic jump, F = 9.3

Figure 6. Hydraulic jump, F = 5.9

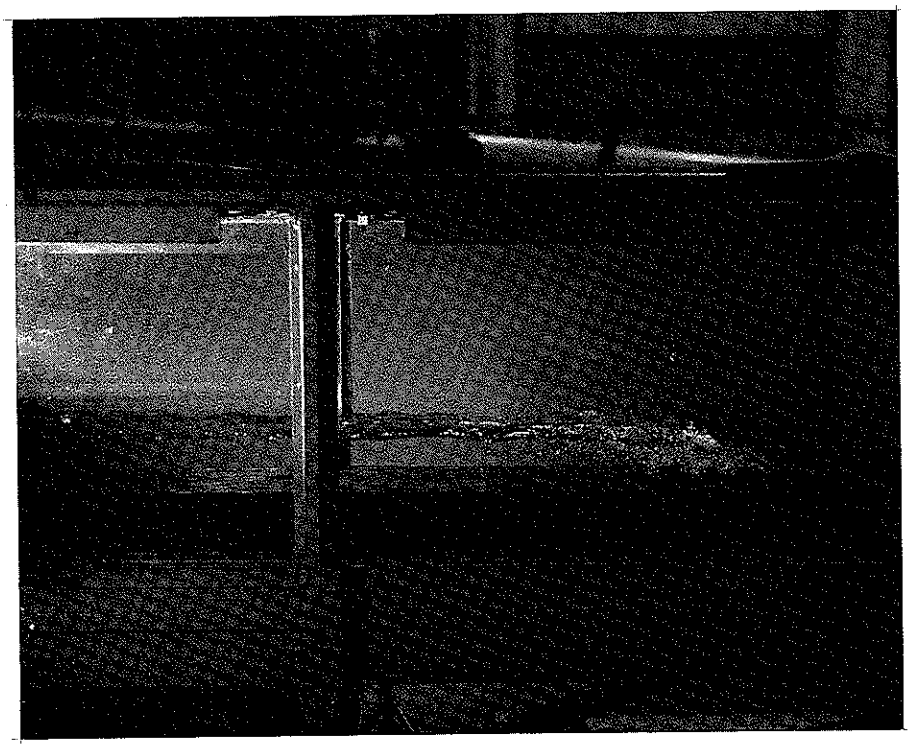

Figure 7. Hydraulic jump, F = 3.3

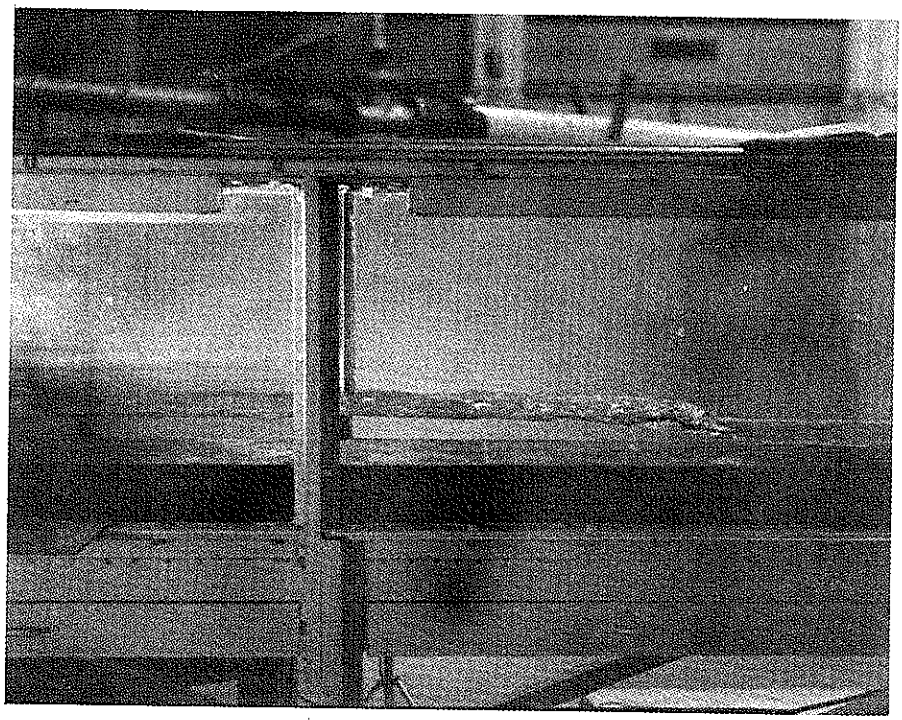

Figure 8. Hydraulic jump, F = 2.4

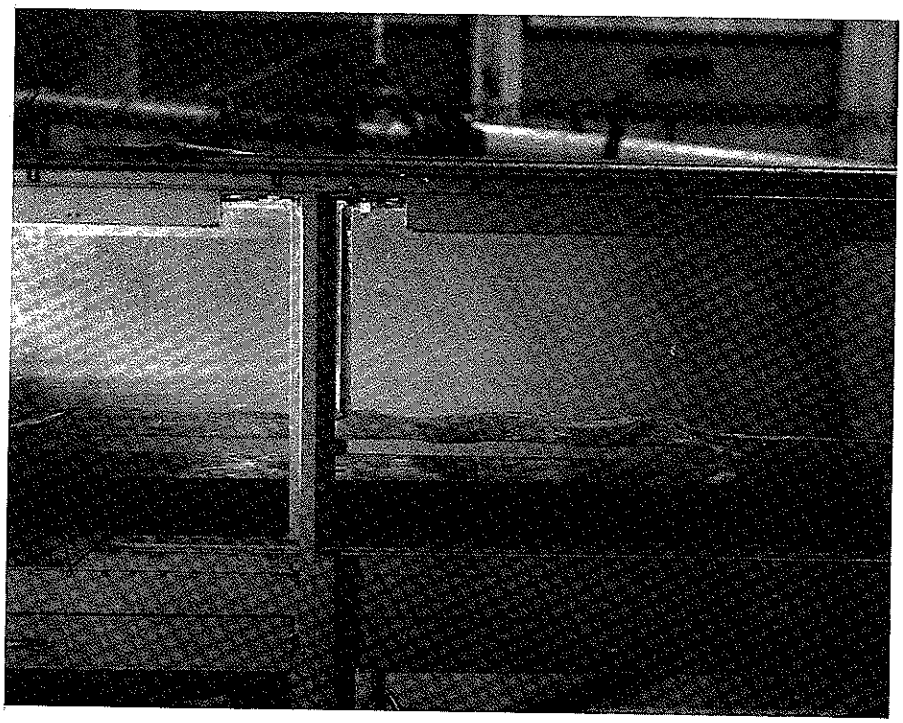

Figure 9. Hydraulic jump, F = 1.8

and give an impression of the different levels of turbulent mixing involved. Unit discharges of 0.462, 0.330, and 0.261 cfs per foot of flume width were tested with jumps from each of the classes.

Procedure

22. The particular flow condition to be tested was established and allowed to stabilize. The velocity of the supercritical flow upstream of the jump was determined using a Pitot-static tube and the relationship

$$V = \frac{Q}{Wd} \tag{8}$$

where

V = velocity upstream of jump, fps

Q = total flow in the flume, cfs

W = flume width, ft

d = depth of flow upstream of jump, ft

Comparison of methods showed an insignificant difference. Equation 8 was used to determine velocity. The Froude number was then computed from these data by

$$F = \frac{V}{(gd)^{1/2}}$$

where

F = Froude number, dimensionless

g = gravitational acceleration = 32.2 ft/sec^2

The depth of flow downstream from the jump (sequent depth) was computed from the equation (Chow 1959)

$$\frac{Y_2}{Y_1} = 1/2 \left[(1 + 8F^2)^{1/2} - 1 \right]$$

where

Y_2 = downstream depth, ft

Y_1 = upstream depth, ft

and checked with direct depth measurements in the flume.

23. The jump length, L, was determined from an empirical relationship (Chow 1959) of L/Y_2 and F. The sampling locations were established by moving downstream from the leading edge of the jump. For most tests, samples were taken at stations A, B, C, and D which were located at the leading edge (Figure 5) and at distances of one, two, and three jump lengths from the leading edge, respectively.

24. Time of flow between stations was determined using conductivity probes and a salt brine. The conductivity probes were placed at the leading edge of the jump and at one of the other specified multiples of the jump length. An "instantaneous" dose of brine was introduced upstream of the jump. The conductivity of the water increased and then decreased as the brine passed the sampling locations. The passing of the brine was recorded on a high-speed strip chart recorder (Figure 10). The lapse time between peaks on the recording was the time of flow between the leading edge and the station being tested. This test was repeated several times at each location to determine a mean travel time between stations.

25. To efficiently and accurately locate sampling stations during a test the following method was used. The sampling pumps were mounted on a carriage which could be rolled along the length of the flume. The sampling system (pumps and carriage) was positioned at the leading edge of the jump (Figure 11). A small c-clamp chocked the rollers to prevent movement of the carriage. Other clamps were placed at multiples of the jump length downstream. When sampling was completed at one station, the clamp chocking the carriage was removed, and the carriage rolled downstream to the next clamp that positioned the sampling system at the correct location.

26. Samples were drawn from the quarter-depths of the tailwater, i.e., at 1/4 and 3/4 of the tailwater depth, to determine if stratified

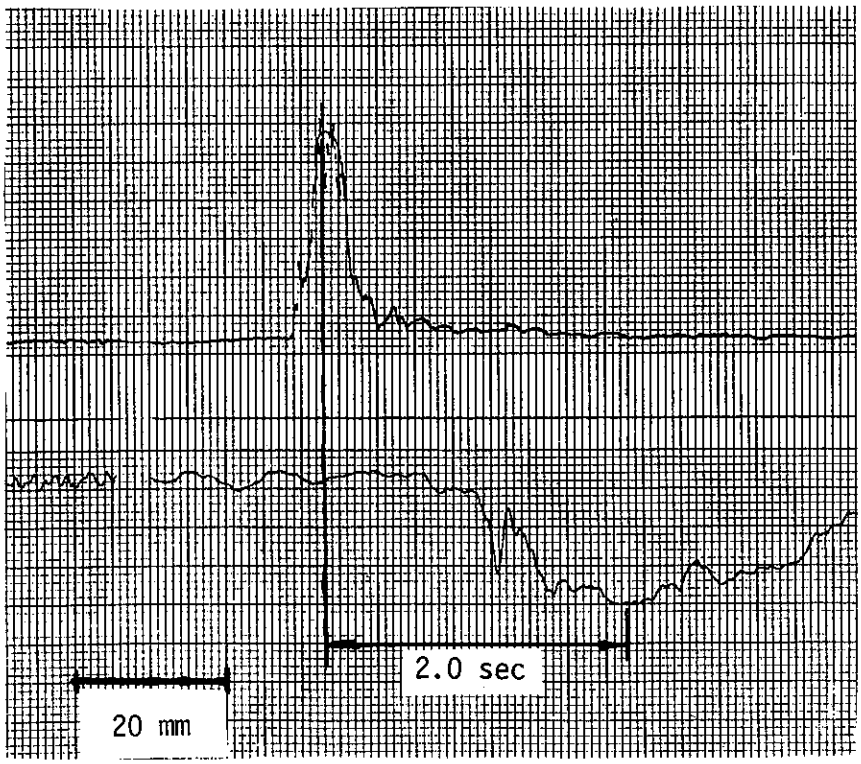

Figure 10. Strip chart recording of conductivity as brine dose passed stations A and C, F = 9.4 , chart speed 20 mm/sec

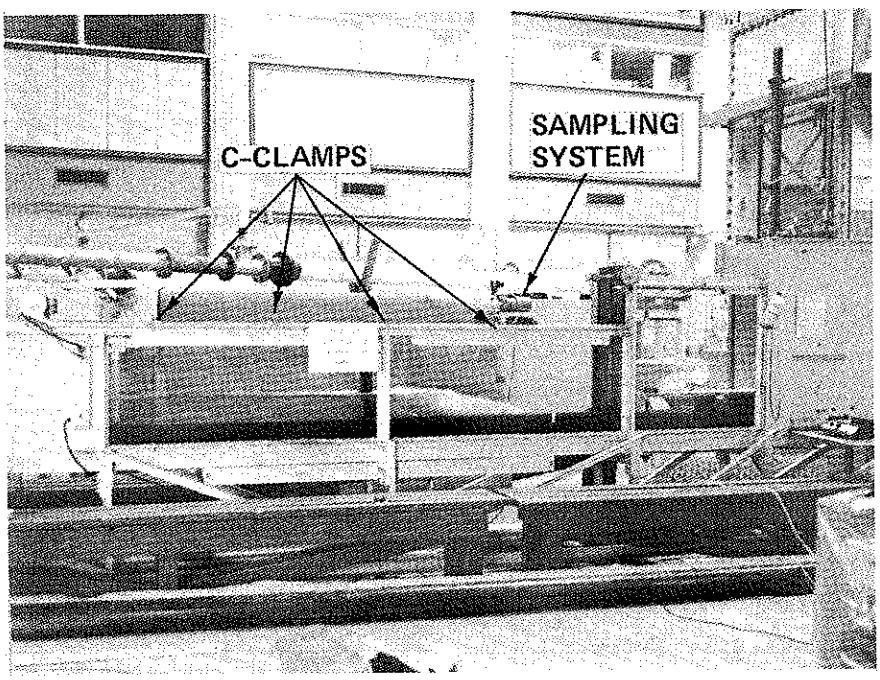

Figure 11. Sampling station location

flow existed in the jump. The sample bottles were equipped with plastic tubing reservoirs (Figure 12) that provided the extra water needed to

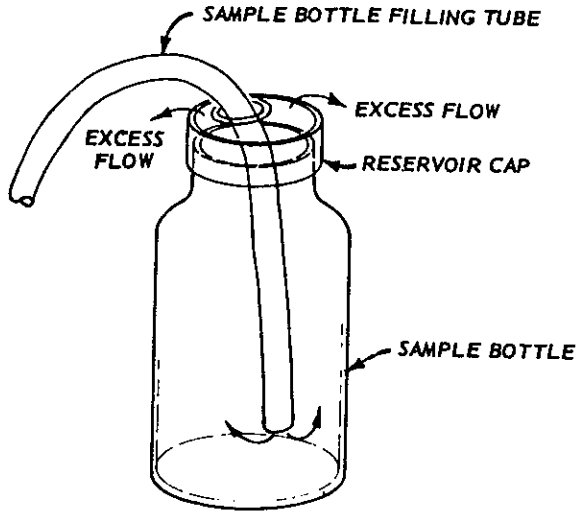

Figure 12. Sample bottle and reservoir cap

assure full sample bottles when the tygon tubes were withdrawn.

27. The tracer mixture was provided by the Georgia Institute of Technology, Nuclear Science Department, in a sealed bottle. The mixture was transferred to a 50-cc glass syringe by using a second syringe to force the dose from the dose bottle into the 50-cc syringe (Figure 13). The 50-cc injection syringe was fitted with a 3-in.-long needle which extended well down into the bottle. The 50-cc syringe needle and a short needle attached to a 100-cc syringe were passed through a rubber stopper. The rubber stopper was fitted into the mouth of the dose bottle (Figure 14). The 100-cc syringe was plunged, forcing the tracers into the 50-cc syringe. This operation successfully prevented krypton loss from the mixture by minimizing air contact with the mixture.

28. When a test was completed, the sample bottles were capped and taped shut with plastic electrical tape. They were placed in water for temperature stability and transported to the laboratory for analysis.

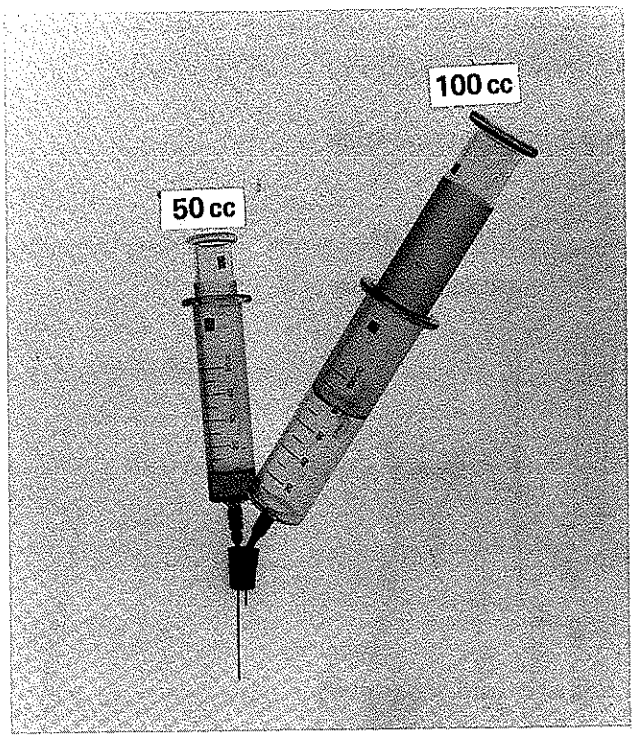

Figure 13. Syringe setup

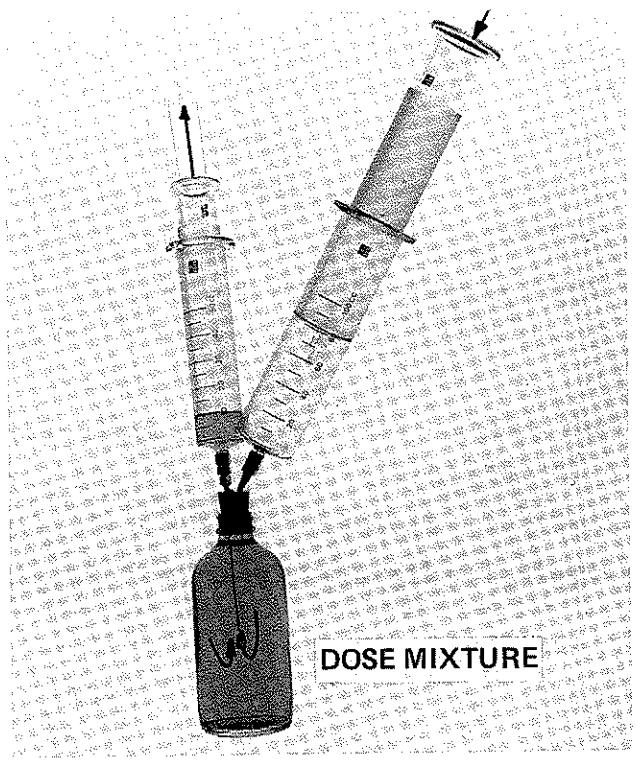

Figure 14. Dose transfer arrangement

Analysis

29. The water samples withdrawn from the flume during each test were prepared for analysis by the method described by Cohen et al. (1968). The krypton-85 concentrations were determined in a liquid scintillation counter. Three replicates of each sample were prepared and cycled through three counting sequences to reduce the effect of any laboratory or counting errors. A fluorometer was used to determine the dye concentrations of the samples.

30. The ratios of krypton-85 to dye and Equation 7 were used to determine the krypton-85 exchange coefficient for the particular jump. Applying a temperature correction (Tsivoglou 1967),

$$K_{ox}^{20} = K_{ox}^{T} 1.022^{(20-T)} \tag{9}$$

where

K_{ox}^{20}, K_{ox}^{T} = oxygen exchange coefficients at temperatures of 20°C and T°C

the exchange coefficient for oxygen at 20°C was computed thus providing a basis for comparison.

PART IV: RESULTS

31. Appendix A presents tables of the krypton-to-dye ratios and other pertinent hydraulic data for the jumps tested. Consider the data from Appendix A, Test 1. The gas fraction remaining in the water at station C was

$$\frac{88.23}{104.70} = 0.843$$

The gas fraction lost to the atmosphere was

$$1.000 - 0.843 = 0.157$$

That is, 15.7 percent of the gas in the water at station A was lost to the atmosphere by the time the flow reached station C, one jump length from A. Similar computations were made for the other tests. By applying Equations 7, 5, and then 9, the exchange coefficients for oxygen were obtained.

32. Table 1 presents the observed gas loss and oxygen exchange coefficients computed from the data for the flume segment extending from the leading edge of the jump to one jump length downstream with a unit discharge in the flume of 0.462 cfs/ft.

33. The data presented in Table 1 indicate that the reaeration rate coefficients, K_{ox}^{20}, vary greatly for replicate tests. This is a direct result of the large variability in observed travel times. For example, the travel time of flow in the hydraulic jump with $9.50 \geq F \geq 9.14$ (4 percent variation) varied from 1.3 to 1.9 seconds (32 percent variation). Time-of-flow measurement error was so great that it prevented using K_{ox} for analysis. Instead, gas loss was evaluated and travel time was not determined for Tests 11-24. Equations 10 and 11 were used to adjust the gas loss data to the common temperature of 20°C:

$$r_T = 1 - L \tag{10}$$

$$\ln r_{20} = \ln r_T (1.022)^{(20-T)} \tag{11}$$

where

r_T , r_{20} = fraction of gas remaining in water at T°C and 20°C

L = fraction of gas lost to atmosphere

T = observed water temperature, °C

Tables 2, 3, and 4 present the gas-loss data after adjustment for temperature for unit discharges of 0.462, 0.330, and 0.261 cfs/ft, respectively.

Table 1

Exchange Coefficients for One Jump Length from A, Unit Discharge = 0.462 cfs/ft

Test	F	Percent* Gas Loss	Travel time-sec	K_{kr}^{T}/sec	K_{ox}^{20}/sec**
1	9.14	15.7	1.93	0.089	0.098
2	9.46	17.5	1.62	0.119	0.129
3	9.50	17.0	1.29	0.145	0.163
4	5.98	11.7	1.37	0.091	0.102
5	6.14	10.0	1.32	0.080	0.090
6	3.34	4.3	0.95	0.046	0.052
7	3.29	1.3	0.99	0.014	0.015
8	2.65	1.8	0.94	0.019	0.018
9	2.33	2.0	0.71	0.028	0.026
10	1.89	0.6	0.47	NA	NA
11	9.24	26.0	NA	NA	NA
12	9.24	25.0	NA	NA	NA

Note: NA = Not available or not taken.
* Not adjusted for temperature.
** Temperature corrected with Equation 9.

Table 2

Gas Loss Data for One Jump Length from Station A, Unit Discharge = 0.462 cfs/ft

Test	F	Percent Gas Loss
1	9.14	14.5
2	9.46	15.9
3	9.5	16.0
4	5.98	11.0
5	6.14	9.4
6	3.34	4.0
7	3.29	1.2
8	2.65	1.7
9	2.33	1.9
10	1.89	NA
11	9.24	27.2
12	9.24	26.2

Table 3

Gas Loss Data for One Jump Length from Station A, Unit Discharge = 0.330 cfs/ft

Test	F	Percent Gas Loss
13	9.28	17.5
14	9.28	19.6
15	6.52	7.1
16	6.52	10.1
17	4.51	6.9
18	4.51	7.9
19	3.35	3.3

Table 4

Gas Loss Data for One Jump Length from Station A, Unit Discharge = 0.261 cfs/ft

Test	F	Percent Gas Loss
20	9.85	11.9
21	9.35	12.6
22	6.23	4.7
23	6.23	6.8
24	3.68	NA

PART V: DISCUSSION

34. Gas loss occurred in the first jump length downstream from the leading edge (region of roller and high turbulence). Farther downstream, gas loss measurements apparently were within the experimental error, as the observed gas "loss" for most tests varied between +4.0 and -4.8 percent for subsequent jump lengths. Gas transfer studies at the Enid Lake outlet works (Tate 1978) indicated similar behavior at the hydraulic jump that occurred in the outlet conduit near the flow control gate. A large fraction of the tracer gas was lost in the hydraulic jump in the conduit. This was expected since a large amount of energy was dissipated in this aerated turbulent region.

35. Several experimenters and researchers (Tsivoglou and Wallace 1972, Krenkel and Orlob 1963), working mostly with streams and rivers, have related gas transfer to energy dissipation. In a hydraulic jump, the energy loss is related to the Froude number of incoming flow. Figures 15, 16, and 17 show plots of gas loss versus Froude number on a semilogarithmic coordinate system for the three unit discharges tested. Gas loss was related to Froude number in a similar manner for each of the unit discharges tested. As energy dissipation and Froude number increased, gas loss increased for a given unit discharge. There was a detection threshold for each unit discharge below which the energy loss was too small to cause any significant gas loss.

36. For two of the high discharge tests at high Froude numbers ($F > 9$) and for the intermediate discharge tests there was more gas loss than expected based on previous tests (Figures 16 and 17). However, least squares regression and statistical analyses (Draper and Smith 1966) indicated insignificant differences in slope regression coefficients for the data plotted in Figures 15, 16, and 17; therefore the lines passing through the data in these figures were drawn on the same slope. Additional tests should be performed to isolate the factors causing the higher gas losses in these tests.

37. The results presented in Figures 15, 16, and 17 clearly demonstrate that a free hydraulic jump can be used to improve water quality

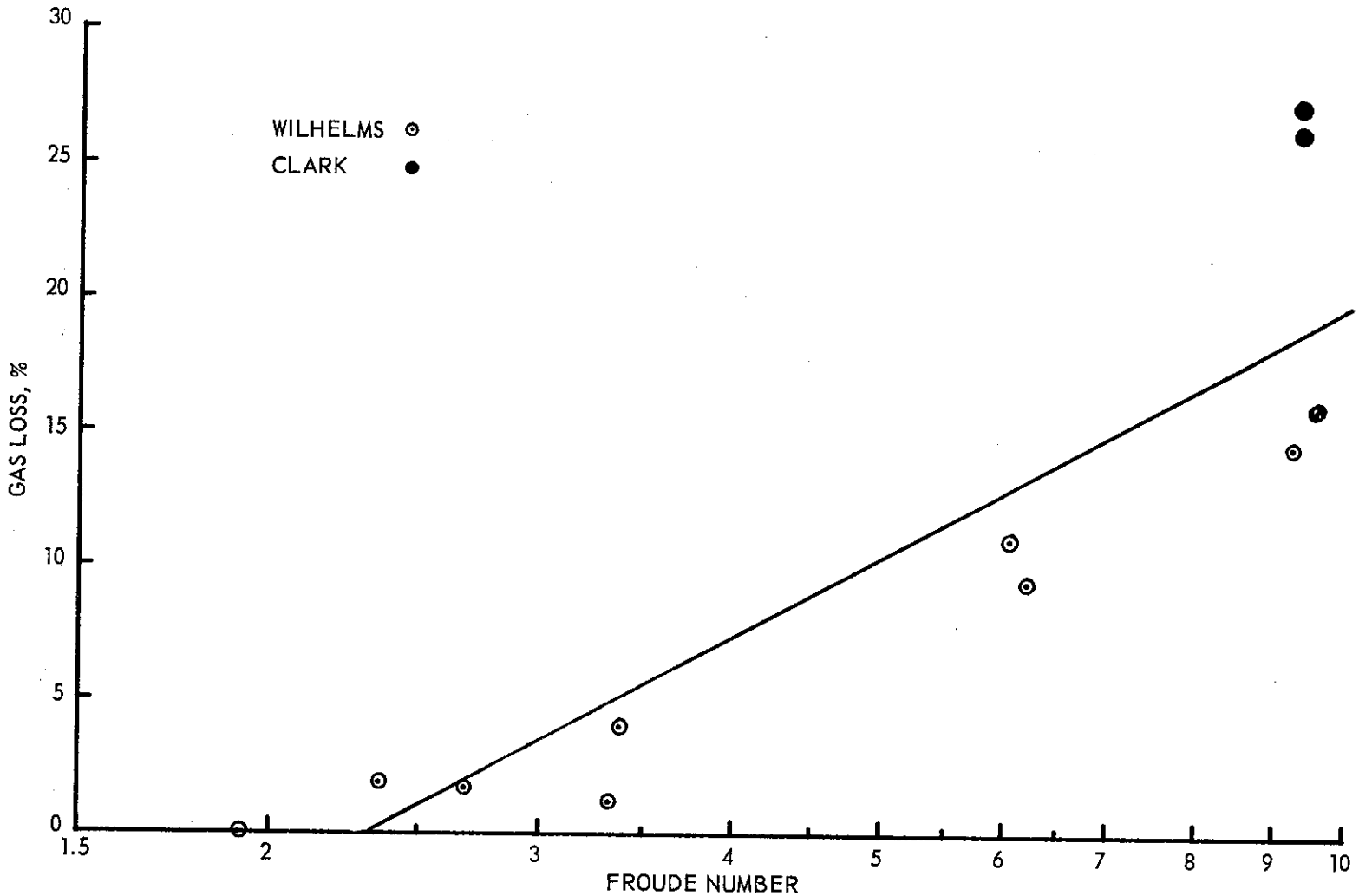

Figure 15. Gas loss versus Froude number, unit discharge = 0.462 cfs/ft

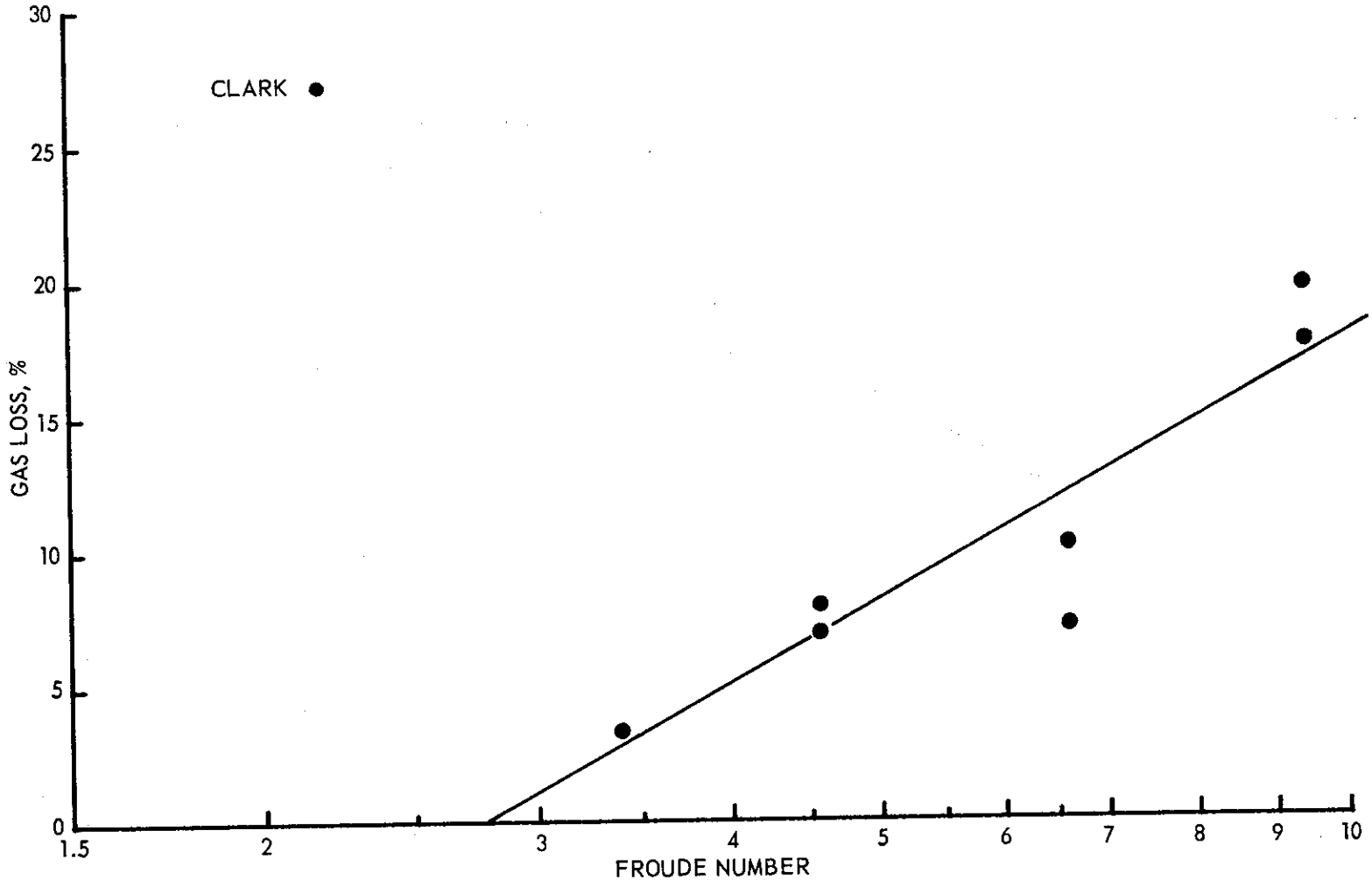

Figure 16. Gas loss versus Froude number, unit discharge = 0.331 cfs/ft

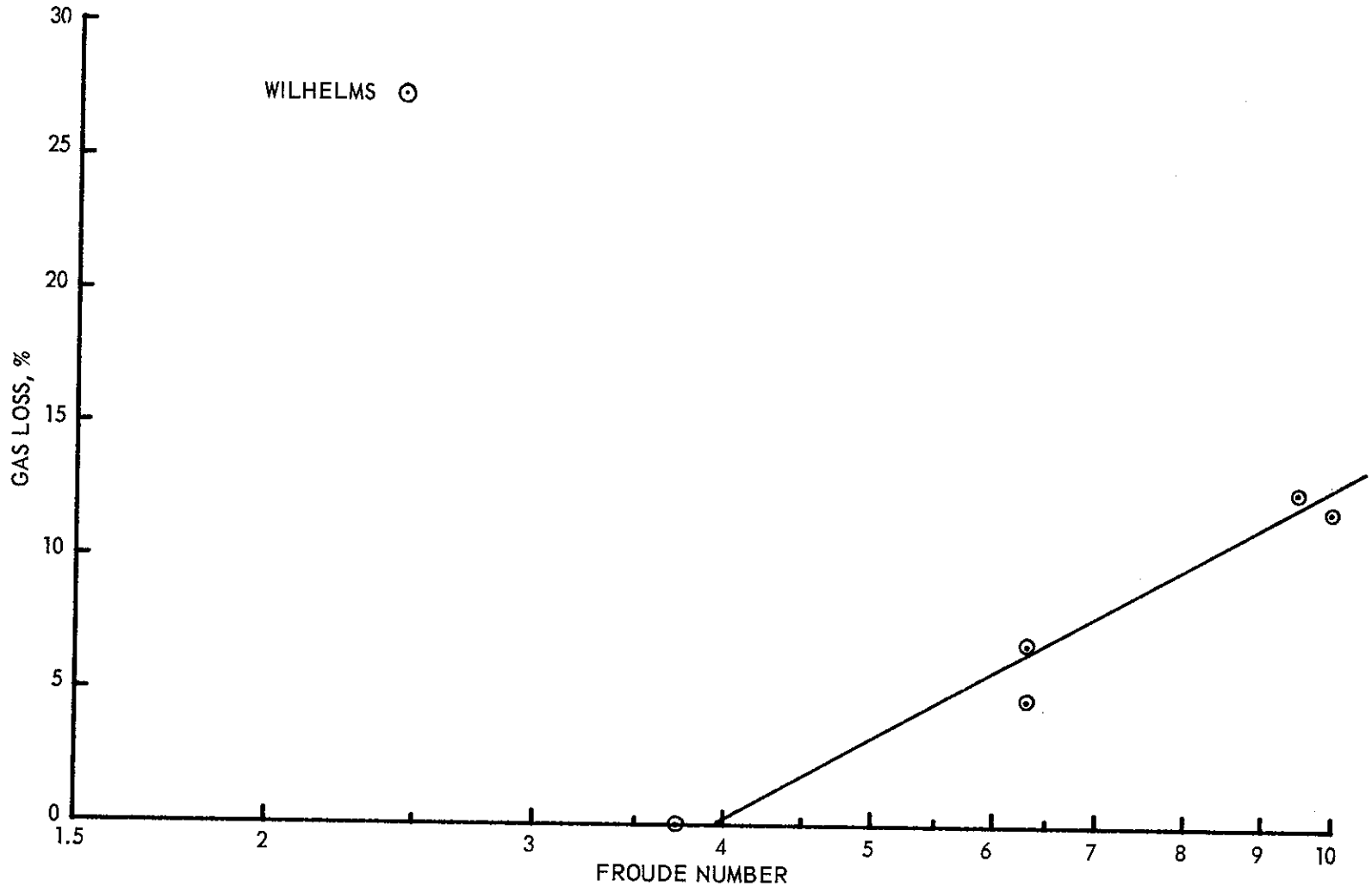

Figure 17. Gas loss versus Froude number, unit discharge = 0.261 cfs/ft

by enhancing gas exchange between the flowing water and the atmosphere. Dissolved gas concentrations in the water tend to equilibrate with atmospheric concentrations during flow through a jump. Consequently, if a DO deficit exists just upstream from a jump, the DO will increase through the jump. The magnitude of the DO uptake will increase with Froude number and unit discharge.

PART VI: CONCLUSIONS AND RECOMMENDATIONS

38. Figure 18 shows a summary of results taken from Figures 15, 16, and 17. This figure shows the relationship of gas loss, unit discharge, and Froude number. These curves are empirical, confined to the experimental and hydraulic conditions tested, and should not be extrapolated beyond the ranges shown. The results presented in Figure 18 can be used to estimate the gas transfer that would occur in hydraulic jumps within the range of operating conditions investigated.

39. Gas loss is related to changes in DO concentrations or deficits through the computations in paragraph 31 and Equations 3, 4, and 5. Thus the results presented above may be used to estimate DO uptake in a hydraulic jump in terms of dimensionless parameters that are typically used to characterize the gas transfer process. The Reynolds number R of flow upstream of the jump is defined by the unit discharge divided by the kinematic viscosity of the water. Consequently, the ratio of upstream-to-downstream deficits can be related to the Froude number and Reynolds number of flow upstream of the jump. Avery and Novak (1975) and Avery et al. (1977) related dissolved oxygen measurements to F and R in the following manner,

$$\frac{D_o}{D} - 1 = 1.0043 \times 10^{-6} F^{2.1} R^{0.75} \tag{12}$$

Figure 19 shows a family of curves that indicate the relations described by Equation 12. Also shown is the range of data over which Equation 12 was developed.

40. Regression analysis of the data collected in this study resulted in the following equation relating oxygen deficit to Froude number and Reynolds number:

$$\frac{D_o}{D} - 1 = 4.924 \times 10^{-8} F^{2.106} R^{1.034} \tag{13}$$

After rearranging to predict D/D_o, the resulting family of curves is shown in Figure 20.

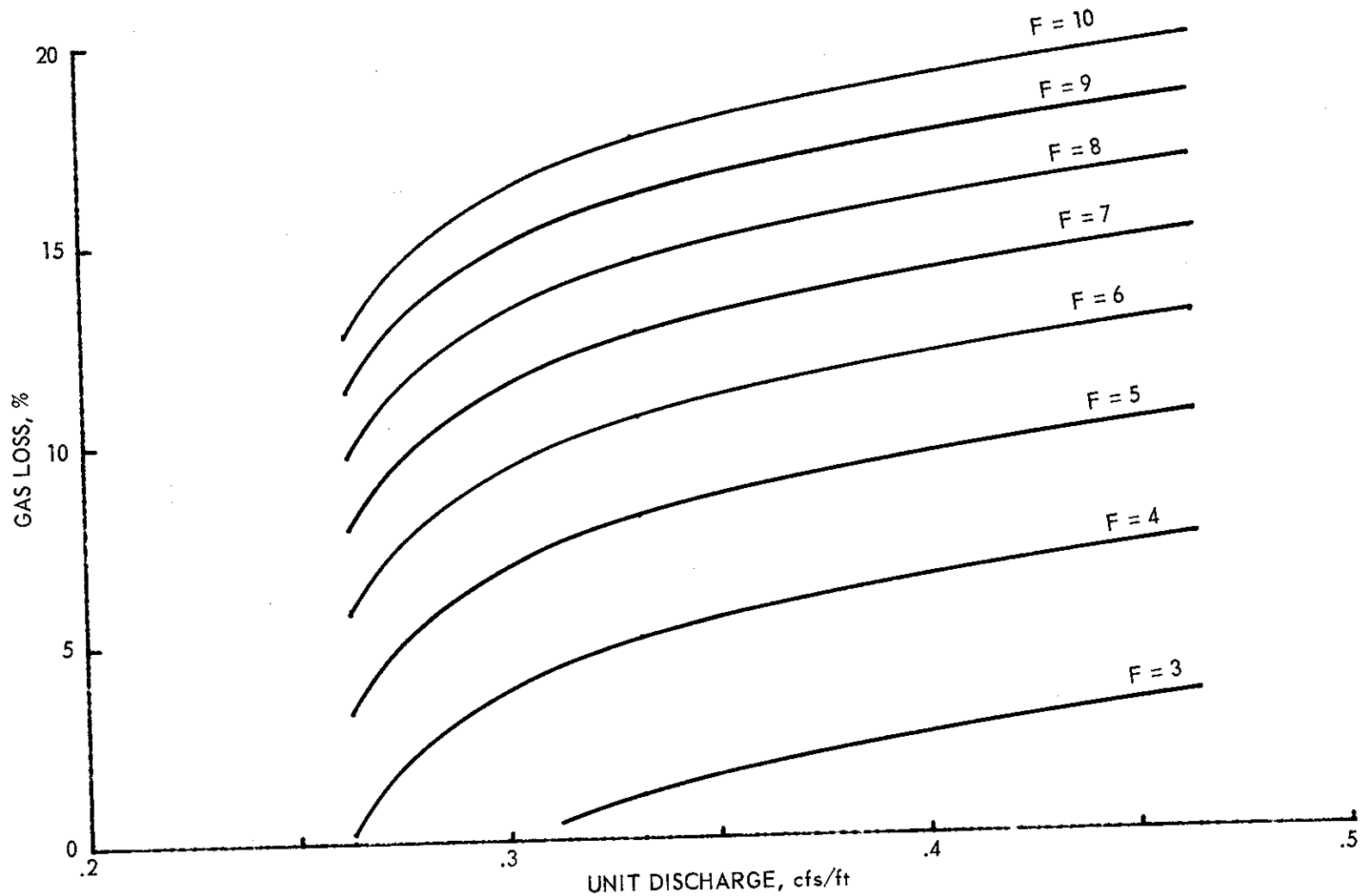

Figure 18. Summary of results taken from Figures 15, 16, and 17

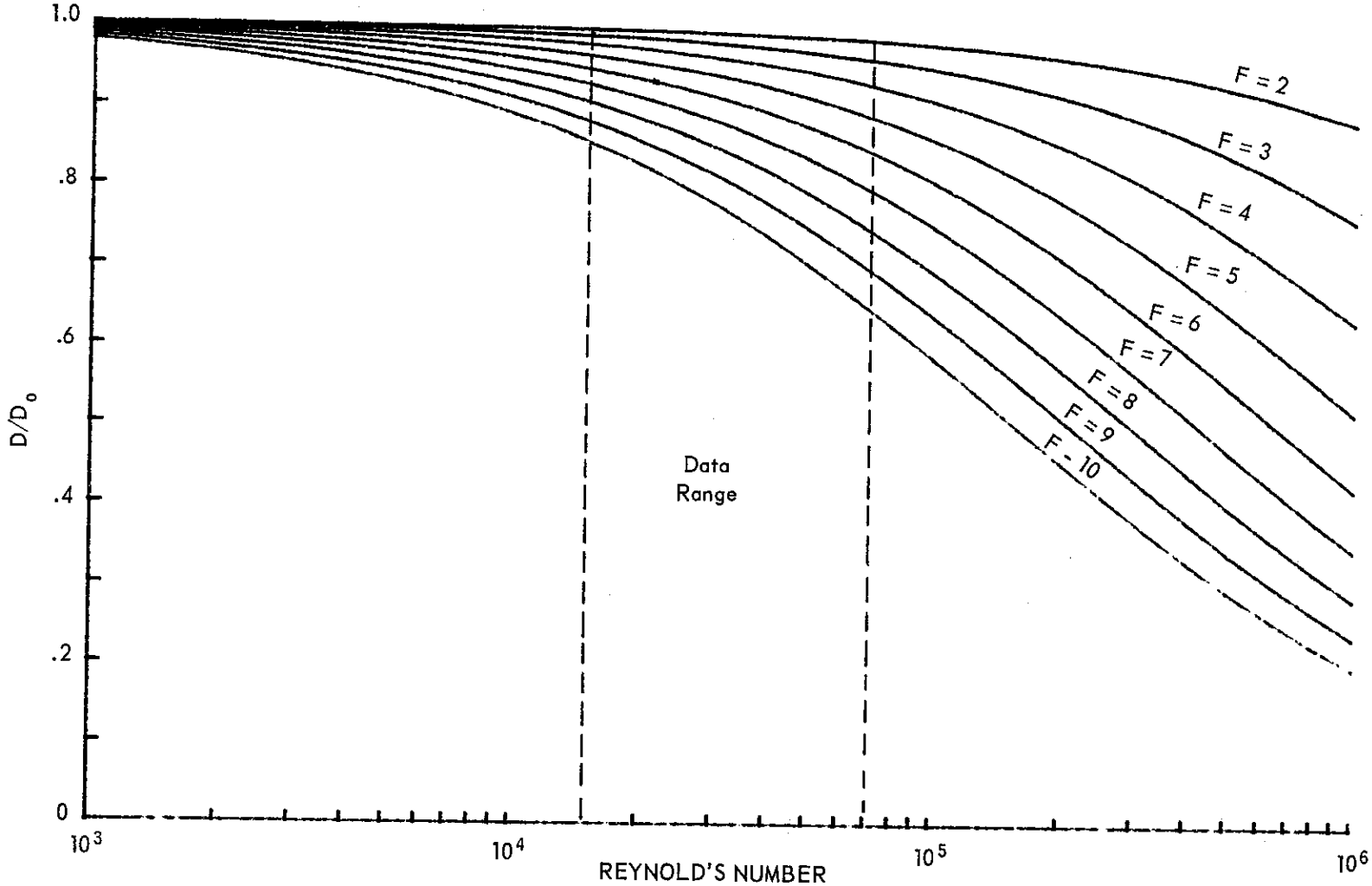

Figure 19. Oxygen transfer in hydraulic jumps (Avery et al. 1977)

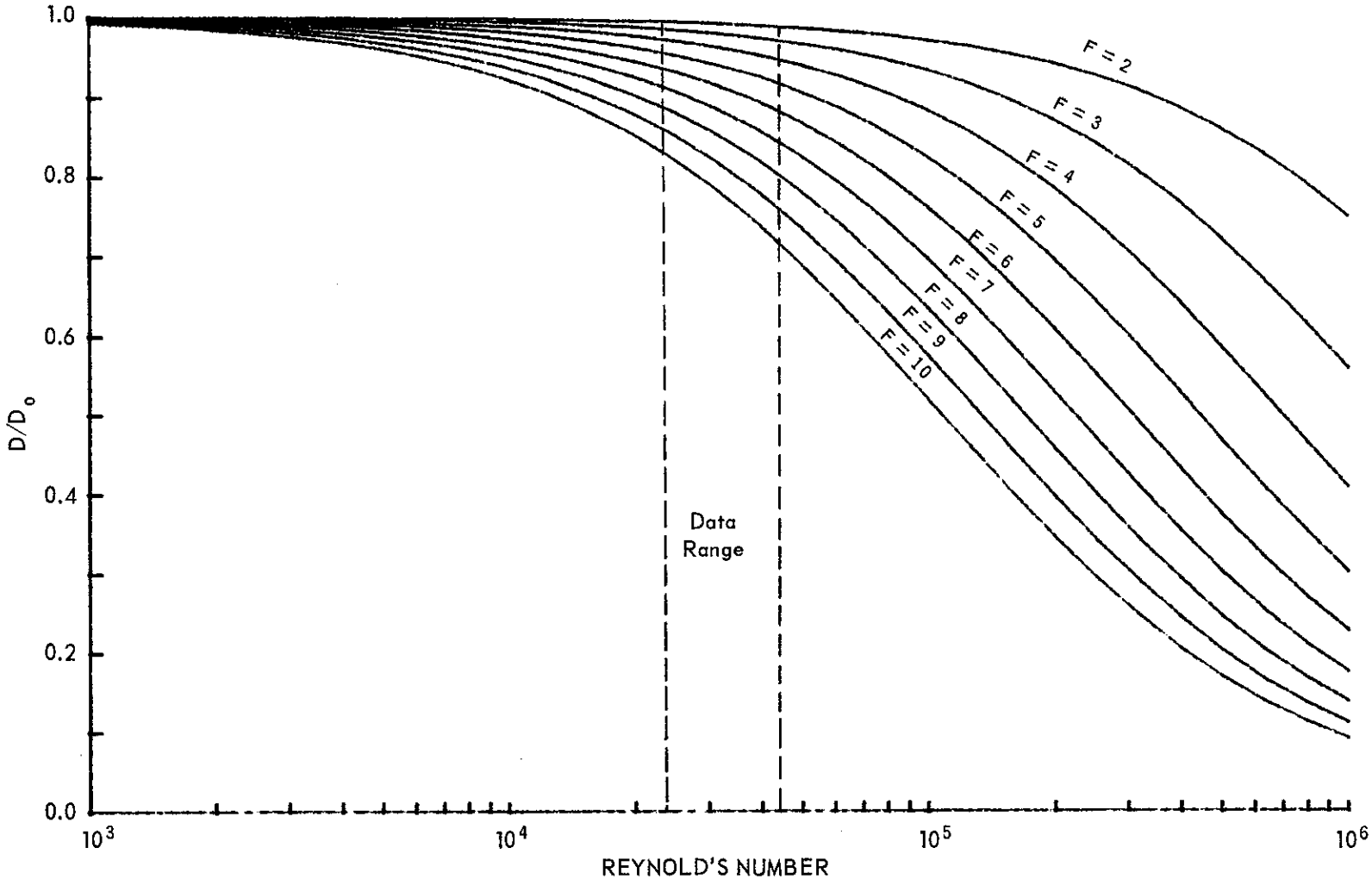

Figure 20. Oxygen transfer in hydraulic jumps (Data reported herein)

41. Initial comparison of Equations 12 and 13 suggests significant differences in deficit predictions. The differences in the coefficients and exponents reflect the result of regression analysis with data for a limited range of Reynolds numbers as indicated in Figures 19 and 20. Additionally, the respective data bases were obtained with different experimental techniques. However, comparing Equations 12 and 13 over the data range with which they were developed (Figure 21) shows only minor differences in predictions. Thus either equation may be used to estimate oxygen uptake for the hydraulic conditions investigated. The major limitation of Equations 12 and 13 is that they were developed over a small range of Reynolds numbers. Prototype Reynolds numbers are typically 10^6 or greater instead of on the order of 10^4 as in this study and Avery's (Avery et al. 1977) investigation. However, Equations 12 and 13 demonstrate that Froude and Reynolds numbers may be used to characterize reaeration in hydraulic jumps. The relationship of F , R , and gas transfer must be further evaluated by increasing the range of Reynolds number to include prototype magnitudes. It is probable that there are critical Reynolds numbers above which gas transfer is insensitive to turbulence described by Reynolds number. It is anticipated that prototypes will respond in a manner similar to those encountered in this investigation and once this relationship is established, quantitative predictive techniques may be available to convert hydraulic model data to prototype equivalents.

42. Further testing is needed to verify the two-dimensionality of gas transfer in hydraulic jumps, i.e., comparison on a unit-discharge basis. Channel bottom and sidewall boundary effects must be evaluated to ascertain their influence on jump turbulence and gas transfer. Other parameters such as amount of entrained air, entrained bubble sizes, bubble detention time in the jump, mass exchange between the roller and the remainder of the jump, and pressure conditions in the jump must be evaluated regarding their influence on the gas transfer process.

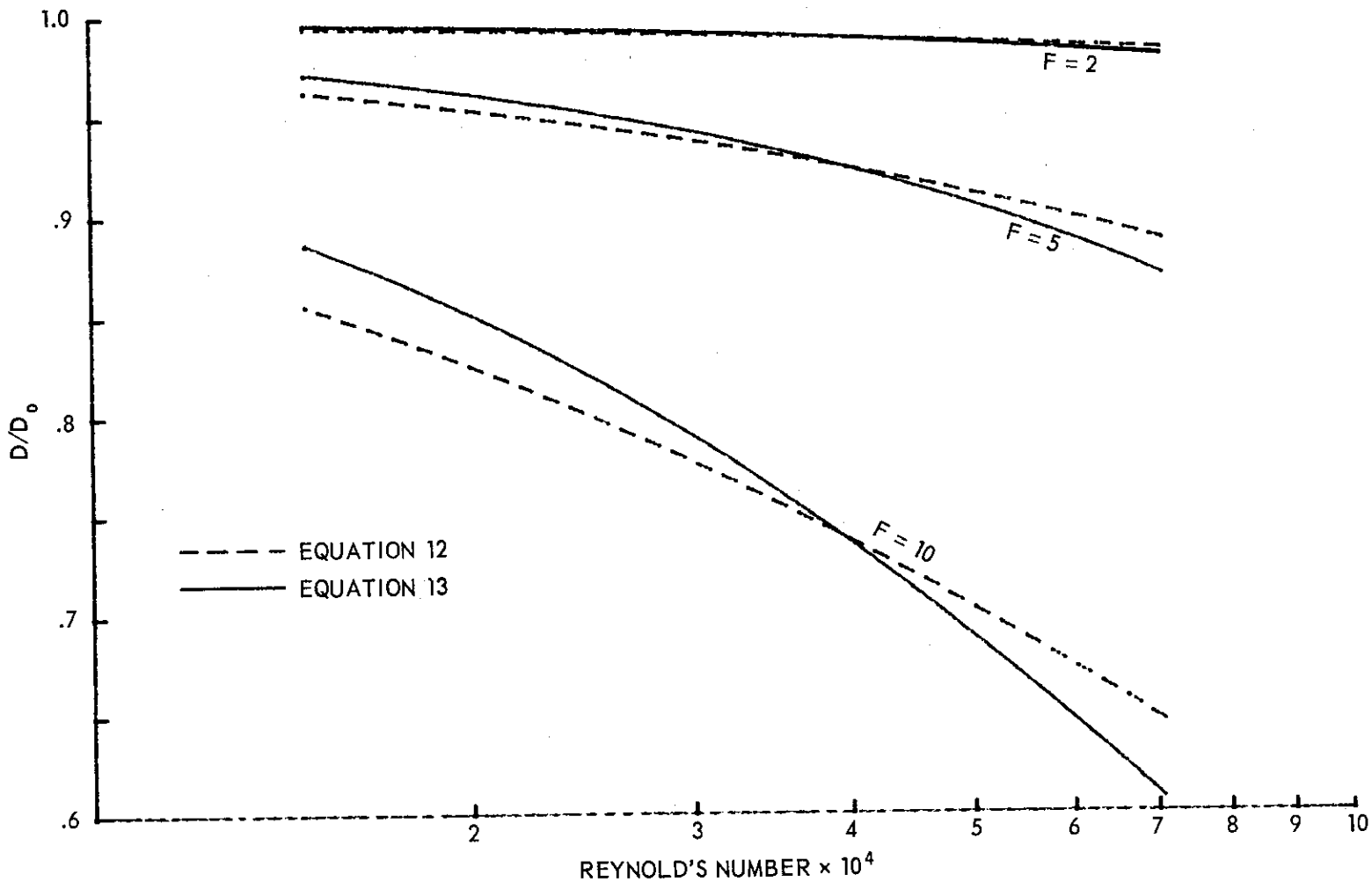

Figure 21. Comparison of Equations 12 and 13 over Avery's (Avery et al. 1977) data range

REFERENCES

Avery, S. T. and Novak, P. 1975. "Oxygen Uptake in Hydraulic Jumps and at Overfalls," Proceedings, XVI Congress of the International Association for Hydraulic Research, Sao Paulo, Brazil.

Avery, S. T., Watson, J. D. and D. M., Novak, P. 1977. "Modeling of Oxygen Transfer from Air Entrained by Solid Jets Entering a Free Water Recipient," Proceedings of XVII Congress, International Association for Hydraulic Research, Baden-Baden, West Germany.

Chow, V. T. 1959. Open Channel Hydraulics, McGraw-Hill, New York.

Cohen, J. B. et al. 1968. "Analytical Method for the Determination of ^{3}H and ^{85}Kr in Aqueous Samples by Liquid Scintillation Techniques," Talanta.

Draper, N. R. and Smith, H. 1966. Applied Regression Analysis, John Wiley and Sons, New York.

Krenkel, P. A. and Orlob, G. T. 1963. "Turbulent Diffusion and the Reaeration Coefficient," Transactions, American Society of Civil Engineers, Vol 125, Part III, Paper No. 3491.

Rathbun, R. E. 1977. "Reaeration Coefficients of Streams - State-of-the-Art," American Society of Civil Engineers, Hydraulics Division Journal, Vol 103, No. HY4.

Tate, C. H. 1978. Unpublished data, U. S. Army Engineers, Waterways Experiment Station, Vicksburg, Miss.

Tsivoglou, E. C. 1967. "Tracer Measurement of Stream Reaeration," Federal Water Pollution Control Administration, Washington, D.C.

Tsivoglou, E. C. and Wallace, J. R. 1972. "Characterization of Stream Reaeration Capacity," EPA-R3-72-012, U. S. Environmental Protection Agency, Washington, D.C.

Tsivoglou, E. C. et al. 1965. "Tracer Measurement of Atmospheric Reaeration: I. Laboratory Studies," Water Pollution Control Federation Journal, Vol 37, No. 10.

Tsivoglou, E. C. et. al. 1968. "Tracer Measurement of Stream Reaeration: II. Field Studies," Water Pollution Control Federation Journal, Vol 37, No. 10.

APPENDIX A
KRYPTON-TO-DYE RATIOS AND PERTINENT DATA FOR HYDRAULIC JUMPS

Table A1

Krypton-to-Dye Ratios

Test 1**

F = 9.14 V = 10.75 fps Y_1 = 0.043 ft L = 3.40 ft

	Station A	Station B	Station C	Station D
Ratio	104.7	84.10	89.70	86.00
	*	84.10	89.80	85.30
	*	67.80	87.40	87.80
	*	70.40	86.00	87.90
Mean:	104.7	76.60	88.23	86.75

Water Temperature: 23.9°C

From	To	Mean Time of Flow, sec
A	B	0.611
A	C	1.928
A	D	4.383

Test 2**

F = 9.46 V = 11.00 fps Y_1 = 0.042 ft L = 3.43 ft

	Station A	Station B	Station C	Station D
Ratio	90.55	61.68	75.36	79.19
	95.57	57.78	76.00	76.28
	90.49	73.73	74.80	74.36
	91.79	71.60	77.74	79.95
Mean:	92.10	66.20	75.98	77.45

Water Temperature: 24.7°C

From	To	Mean Travel Time, sec
A	B	0.53
A	C	1.62
A	D	3.96

* Data not available or not taken.
** Stations located one-half jump length apart.

Table A1 (Continued)

Test 3**

F = 9.5 V = 11.00 fps Y_1 = 0.042 ft L = 3.31 ft

	Station A	Station B	Station C	Station D
	75.03	*	60.89	61.00
	74.18	*	61.59	61.26
Ratio	*	*	62.59	59.84
	*	*	62.53	62.36
Mean:	74.61		61.90	61.12

Water Temperature: 23.15°C

From	To	Mean Travel Time, sec
A	B	0.70
A	C	1.29
A	D	2.87

Test 4

F = 5.98 V = 8.11 fps Y_1 = 0.057 ft L = 2.76 ft

	Station A	Station B	Station C	Station D
	91.09	79.70	80.21	80.51
	92.11	82.72	80.49	80.65
Ratio	91.73	*	82.89	83.35
	92.85	*	81.82	83.14
Mean:	91.95	81.21	81.36	81.91

Water Temperature: 23.2°C

From	To	Mean Travel Time, sec
A	B	1.37
A	C	2.80
A	D	5.84

Table A1 (Continued)

Test 5

F = 6.14 V = 8.25 fps Y_1 = 0.056 ft L = 2.68 ft

	Station A	Station B	Station C	Station D
	79.61	73.28	74.11	72.71
	80.60	73.61	74.82	72.53
Ratio	80.31	71.54	72.55	71.83
	83.35	72.94	71.72	*
Mean:	80.97	72.85	73.30	72.35

Water Temperature: 23.15°C

From	To	Mean Travel Time, t , sec
A	B	1.32
A	C	3.70
A	D	5.82

Test 6

F = 3.34 V = 5.50 fps Y_1 = 0.084 ft L = 1.90 ft

	Station A	Station B	Station C	Station D
	96.54	90.46	93.46	92.79
	94.43	91.09	91.54	92.01
Ratio	97.04	92.62	93.31	90.61
	97.64	94.88	93.90	91.61
Mean:	96.42	92.26	93.06	91.76

Water Temperature: 23.4°C

From	To	Mean Travel Time, t , sec
A	B	0.95
A	C	1.96
A	D	3.57

Table A1 (Continued)

Test 7

F = 3.29 V = 5.44 fps Y_1 = 0.085 ft L = 1.93 ft

	Station A	Station B	Station C	Station D
Ratio	91.64	90.92	*	93.11
	95.64	93.16	*	93.09
	93.47	92.82	*	92.19
	93.12	91.92	*	90.54
Mean:	93.47	92.21		92.23

Water Temperature: 23.0°C

From	To	Mean Travel Time, t , sec
A	B	0.99
A	C	*
A	D	4.17

Test 8

F = 2.65 V = 4.71 fps Y_1 = 0.098 ft L = 1.68 ft

	Station A	Station B	Station C	Station D
Ratio	94.72	95.36	91.39	92.07
	95.15	*	91.64	89.12
	96.13	92.63	93.26	92.54
	95.34	92.85	90.52	93.22
Mean:	95.33	93.61	91.70	91.74

Water Temperature: 23.4°C

From	To	Mean Travel Time, t , sec
A	B	0.94
A	C	2.25
A	D	3.57

Table A1 (Continued)

Test 9

F = 2.33 V = 4.32 fps Y_1 = 0.107 ft L = 1.41 ft

	Station A	Station B	Station C	Station D
Ratio	87.75	84.51	81.81	86.37
	89.06	85.99	84.19	83.16
	86.07	84.80	86.97	83.20
	84.46	85.03	86.52	84.94
Mean:	86.83	85.08	84.87	84.42

Water Temperature: 23.4°C

From	To	Mean Travel Time, t , sec
A	B	0.71
A	C	1.42
A	D	2.61

Test 10

F = 1.89 V = 3.76 fps Y_1 = 0.123 ft L = 1.11 ft

	Station A	Station B	Station C	Station D
Ratio	19.46	19.57	20.14	20.09
	19.71	19.34	19.63	19.67
	*	19.54	19.60	19.89
	*	*	19.24	18.37
Mean:	19.59	19.48	19.65	19.51

Water Temperature: 22.8°C

From	To	Mean Travel Time, t , sec
A	B	0.47
A	C	0.99
A	D	1.48

Table A1 (Continued)

Test 11**

F = 9.24 V = 10.58 fps Y_1 = 0.041 ft L = 3.12 ft

	Station A	Station B	Station C	Station D
Ratio	73.2	50.4	59.3	*
	*	54.7	56.7	*
	*	57.0	52.3	*
	74.6	53.0	52.6	*
Mean:	74.2	53.8	55.2	

Water Temperature: 17.5°C

Test 12**

F = 9.24 V = 10.58 fps Y_1 = 0.041 ft L = 3.12 ft

	Station A	Station B	Station C	Station D
Ratio	69.5	53.3	51.1	*
	*	52.7	50.7	*
	*	56.2	55.6	*
	72.9	53.7	56.4	*
Mean:	71.2	53.7	53.2	

Water Temperature: 17.5°C

Test 13

F = 9.28 V = 9.71 fps Y_1 = 0.034 ft L = 2.64 ft

	Station A	Station B	Station C	Station D
Ratio	37.3	32.1	35.2	*
	43.4	33.6	34.1	*
	37.3	28.1	30.7	*
	41.4	38.9	32.8	*
Mean:	39.8	33.2	33.1	

Water Temperature: 18.4°C

Table A1 (Continued)

Test 14

F = 9.28 V = 9.71 fps Y_1 = 0.034 ft L = 2.64 ft

	Station A	Station B	Station C	Station D
	*	33.0	33.9	*
	47.5	32.6	38.1	*
Ratio	42.0	30.0	34.5	*
	46.6	31.3	38.5	*
Mean:	45.0	31.7	36.3	

Water Temperature: 18.4°C

Test 15

F = 6.52 V = 7.67 fps Y_1 = 0.043 ft L = 2.29 ft

	Station A	Station B	Station C	Station D
	69.7	59.0	67.3	*
	70.5	76.1	64.6	*
Ratio	71.5	61.2	68.0	*
	75.1	69.3	67.9	*
Mean:	71.7	64.2	66.9	

Water Temperature: 19.5°C

Test 16

F = 6.52 V = 7.67 fps Y_1 = 0.043 ft L = 2.29 ft

	Station A	Station B	Station C	Station D
	62.6	55.2	55.3	*
	63.4	54.6	55.6	*
Ratio	63.6	51.7	56.4	*
	63.0	54.8	59.3	*
Mean:	63.2	54.1	56.7	

Water Temperature: 19.5°C

Table A1 (Continued)

Test 17

F = 4.51 V = 6.00 fps Y_1 = 0.055 ft L = 1.93 ft

	Station A	Station B	Station C	Station D
Ratio	*	55.2	55.9	*
	61.8	57.5	54.1	*
	59.0	*	57.8	*
	60.4	58.3	*	*
Mean:	60.4	56.9	55.9	

Water Temperature: 20.6°C

Test 18

F = 4.51 V = 6.00 fps Y_1 = 0.055 ft L = 1.93 ft

	Station A	Station B	Station C	Station D
Ratio	*	57.6	55.9	*
	59.9	59.0	53.8	*
	57.5	53.7	53.4	*
	59.7	58.9	53.8	*
Mean:	59.0	57.3	54.2	

Water Temperature: 20.6°C

Test 19

F = 3.35 V = 4.93 fps Y_1 = 0.067 ft L = 1.58 ft

	Station A	Station B	Station C	Station D
Ratio	46.8	51.7	47.6	*
	51.1	49.5	53.8	*
	49.3	46.9	47.2	*
	53.2	48.9	45.5	*
Mean:	50.2	49.3	48.5	

Water Temperature: 20.8°C

Table A1 (Continued)

Test 20

F = 9.85 V = 9.36 fps Y_1 = 0.028 ft L = 2.19 ft

	Station A	Station B	Station C	Station D
Ratio	112.03	99.75	96.29	98.81
	112.64	97.49	96.75	99.14
	110.48	94.01	97.21	96.67
	110.95	99.47	97.03	97.74
Mean:	111.52	97.68	96.82	98.09

Water Temperature: 22.2°C

Test 21

F = 9.35 V = 9.03 fps Y_1 = 0.029 ft L = 2.27 ft

	Station A	Station B	Station C	Station D
Ratio	112.04	99.09	98.82	96.12
	115.95	98.15	98.05	94.89
	*	98.29	97.65	96.00
	112.98	99.18	99.31	96.14
Mean:	113.66	98.68	98.46	95.79

Water Temperature: 22.2°C

Test 22

F = 6.23 V = 6.89 fps Y_1 = 0.038 ft L = 1.93 ft

	Station A	Station B	Station C	Station D
Ratio	89.79	84.75	84.43	*
	88.61	85.25	83.61	*
	88.53	82.76	83.88	*
	89.24	85.78	84.28	*
Mean:	89.04	84.64	84.05	

Water Temperature: 22.2°C

Table A1 (Concluded)

Test 23

F = 6.23 V = 6.89 fps Y_1 = 0.038 ft L = 1.92 ft

	Station			
	A	B	C	D
	92.41	87.28	87.72	*
	95.58	88.42	87.63	*
Ratio	*	86.32	88.87	*
	92.02	88.55	88.39	*
Mean:	94.34	87.64	88.15	

Water Temperature: 22.1°C

Test 24

F = 3.68 V = 4.85 fps Y_1 = 0.054 ft L = 1.46 ft

	Station			
	A	B	C	D
	89.95	89.70	86.64	*
	97.61	91.61	89.10	*
Ratio	89.77	89.22	85.66	*
	92.44	89.94	85.35	*
Mean:	89.94	90.12	86.69	

Water Temperature: 22.2°C

In accordance with letter from DAEN-RDC, DAEN-ASI dated 22 July 1977, Subject: Facsimile Catalog Cards for Laboratory Technical Publications, a facsimile catalog card in Library of Congress MARC format is reproduced below.

Gas transfer in hydraulic jumps : final report / by Steven C. Wilhelms ... [et al]. (School of Civil Engineering, Georgia Institute of Technology). -- Vicksburg, Miss. : U.S. Army Engineer Waterways Experiment Station ; Springfield, Va. : available from NTIS, [1981].

39, 11 p. : ill. ; 27 cm. -- (Technical report / U.S. Army Engineer Waterways Experiment Station ; E-81-10)

Cover title.

"July 1981."

"Prepared for Office, Chief of Engineers, U.S. Army under Contract No. DACW-39-77-C-0079 (EWQOS Work Unit III A.2)."

"Monitored by Hydraulics Laboratory, U.S. Army Engineer Waterways Experiment Station, Vicksburg, Miss."

At head of title: Environmental and Water Quality Operational Studies.

Gas transfer in hydraulic jumps : ... 1981.
(Card 2)

Bibliography: p. 39.

1. Gases. 2. Hydraulic jump. 3. Radioactive tracers. I. Georgia Institute of Technology. School of Civil Engineering. II. United States. Army. Corps of Engineers. Office of the Chief of Engineers. III. U.S. Army Engineer Waterways Experiment Station. Hydraulics Laboratory. IV. Environmental and Water Quality Operational Studies. V. Series: Technical report (U.S. Army Engineer Waterways Experiment Station) ; E-81-10.
TA7.W34 no.E-81-10